and salt contrast between the North Pacific and Southern Ocean would have been the sudden onset of deep convection in the North Pacific. Bottom waters formed would have filled deep Pacific basins and flowed through the Indonesian passage into the eastern Indian Ocean basin, and the locus of deep-water formation along Antarctica would have shoaled (*16*).

How would methane hydrate dissociation and an abrupt change in ocean circulation have affected climate? The injection of 2000 Gt of CH_4 into the oceans over ~10,000 years (the amount necessary to drive the $\delta^{13}C$ excursion) would have been insufficient to raise atmospheric CO_2 concentrations enough to drive whole-ocean warming of 4 to 5°C. The radiative forcing associated with a 70- to 160-ppmv increase in CO_2 would have caused only ~1°C warming (*21*), and therefore the clathrate hypothesis necessitates still unresolved climatic feedbacks to amplify and sustain PETM warmth.

The abrupt switch to convection in the North Pacific is modeled to have warmed the deep ocean by up to 3 to 5°C (Fig. 1) (*16*) and could have driven the PETM by maintaining high levels of atmospheric CO_2 and water vapor. Circulation-induced ocean warming could have driven additional increases in atmospheric CO_2 by destabilizing methane hydrates in deep ocean sediments (*16*). The solubility of CO_2 in seawater would also have decreased because of temperature and salinity changes, promoting higher atmospheric CO_2. Tropical ocean warming would have also promoted a more vigorous hydrologic cycle, higher evaporation rates, and saturation vapor pressures, resulting in increased levels of atmospheric water vapor (*22*), consistent with proxy data for surface water salinity (*7*, *8*) and humidity (*23*, *24*) across the PETM. The added radiative absorption from water vapor would have heightened the sensitivity of surface temperatures to rising atmospheric CO_2 and CH_4 concentrations, providing a strong positive feedback to warming (*25*, *26*). The eventual sequestration of carbon through the biologic pump (*17*), terrestrial productivity (*27*), and weathering (*28*) would have resulted in global cooling over ~100,000 to 200,000 years. Associated temperature and hydrologic cycle changes would have driven a return to deep sinking in the Southern Hemisphere and shutdown of convection in the North Pacific (*16*).

References and Notes

1. J. P. Kennett, L. D. Stott, *Nature* **353**, 225 (1991).
2. E. Thomas, N. J. Shackleton, in *Correlation of the Early Paleogene in Northwest Europe*, R. W. O. Knox, R. M. Corfield, R. E. Dunay, Eds. (Geological Society Special Publication 101, London, 1996), pp. 401–441.
3. P. L. Koch, J. C. Zachos, P. D. Gingerich, *Nature* **358**, 319 (1992).
4. G. R. Dickens, J. R. O'Neil, D. C. Rea, R. M. Owen, *Paleoceanography* **10**, 965 (1995).
5. G. R. Dickens, M. M. Castillo, J. C. G. Walker, *Geology* **25**, 259 (1997).
6. G. A. Schmidt, D. T. Shindell, *Paleoceanography* **18**, 10.1029/2002PA000757 (2003).
7. A. Tripati, H. Elderfield, *Geochem. Geophys. Geosyst.* **5**, 10.1029/2003GC000631 (2004).
8. J. Zachos *et al.*, *Science* **302**, 1551 (2003).
9. We analyzed *Oridorsalis umbonatus, Nuttallides truempyi*, and *Cibicidoides* spp. benthic taxa that have previously been used to reconstruct low-resolution T_B records for the Cenozoic and high-resolution records across the Eocene-Oligocene boundary (*11*). Seawater Mg/Ca can be considered constant over the duration of the PETM, because of the relatively long oceanic residence times of Ca (~10^6 years) and Mg (10^7 years) (*29*). The magnitude of warming calculated is therefore independent of seawater Mg/Ca ratio used. Absolute temperatures were calculated with current estimates for taxon-specific pre-exponential constants (*30*) and reconstructions of seawater Mg/Ca for 55 Ma (3.1 mmol/mol) (*31*).
10. Materials and methods are available as supporting material on *Science* Online.
11. C. Lear, H. Elderfield, P. Wilson, *Science* **287**, 269 (2000).
12. Shipboard Scientific Party, "Arctic Coring Expedition (ACEX): Paleoceanographic and tectonic evolution of the central Arctic Ocean" (Integrated Ocean Drilling Program Preliminary Report 302, ECORD, 2005), available at www.ecord.org/exp/acex/302PR.html.
13. D. K. Pak, K. G. Miller, *Paleoceanography* **7**, 405 (1992).
14. R. Corfield, J. Cartlidge, *Terra Nova* **4**, 443 (1992).
15. K. Miller, R. Fairbanks, G. Mountain, *Paleoceanography* **2**, 1 (1987).
16. K. L. Bice, J. Marotzke, *Paleoceanography* **17**, 9 (2002).
17. H. Stoll, S. Bains, *Paleoceanography* **18**, 10.1029/2002PA000875 (2003).
18. D. J. Thomas, T. J. Bralower, C. E. Jones, *Earth Planet. Sci. Lett.* **209**, 309 (2003).
19. D. J. Thomas, J. C. Zachos, T. J. Bralower, E. Thomas, S. Bohaty, *Geology* **30**, 1067 (2002).
20. R. W. Knox, in *Late Paleocene-Early Eocene Climatic and Biotic Events in the Marine and Terrestrial Record*, M. P. Aubry, S. G. Lucas, W. A. Berggren, Eds. (Columbia Univ. Press, New York, 1998), pp. 91–102.
21. H. Rennsen, C. J. Beefs, T. Fichefet, H. Goosse, D. Kroon, *Paleoceanography* **19**, 10.1029/2003PA000968 (2004).
22. A. Inamdar, V. Ramanathan, *J. Geophys. Res.* **103**, 32177 (1998).
23. C. Robert, J. P. Kennett, *Geology* **22**, 211 (1994).
24. G. J. Bowen, D. J. Beerling, P. L. Koch, J. C. Zachos, T. Quattlebaum, *Nature* **432**, 495 (2004).
25. S. Manabe, R. T. Wetherald, *J. Atmos. Sci.* **24**, 241 (1967).
26. D. Rind *et al.*, *Nature* **349**, 500 (1991).
27. D. J. Beerling, *Palaeogeogr. Palaeoclimatol. Palaeoecol.* **161**, 395 (2000).
28. G. Ravizza, R. N. Norris, J. Blusztajn, M. P. Aubry, *Paleoceanography* **16**, 155 (2001).
29. W. S. Broecker, T. H. Peng, *Tracers in the Sea* (Eldigio, Palisades, NY, 1982).
30. C. Lear, Y. Rosenthal, N. Slowey, *Geochim. Cosmochim. Acta* **66**, 3375 (2002).
31. B. Wilkinson, T. Algeo, *Am. J. Sci.* **289**, 1158 (1989).

32. We thank W. Broecker for discussions; K. Bice, M. Bickle, S. Crowhurst, and A. Piotrowski for thoughtful reviews; R. Eagle for his support and advice; P. Rumford, B. Horan, and Gulf Coast Ocean Drilling Program Repository staff for provision of samples; and L. Booth, P. Ferretti, and M. Greaves for their invaluable technical help. This research used samples and data provided by the Ocean Drilling Program (ODP). Supported by the Comer Foundation.

Supporting Online Material

www.sciencemag.org/cgi/content/full/308/5730/1894/DC1
Materials and Methods
Figs. S1 to S3
Tables S1 to S3
References and Notes

27 December 2004; accepted 20 May 2005
10.1126/science.1109202

Snowfall-Driven Growth in East Antarctic Ice Sheet Mitigates Recent Sea-Level Rise

Curt H. Davis,[1]* Yonghong Li,[1] Joseph R. McConnell,[2] Markus M. Frey,[3] Edward Hanna[4]

Satellite radar altimetry measurements indicate that the East Antarctic ice-sheet interior north of 81.6°S increased in mass by 45 ± 7 billion metric tons per year from 1992 to 2003. Comparisons with contemporaneous meteorological model snowfall estimates suggest that the gain in mass was associated with increased precipitation. A gain of this magnitude is enough to slow sea-level rise by 0.12 ± 0.02 millimeters per year.

Recent studies report substantial contributions from the Greenland (*1*, *2*) and Antarctic (*3*, *4*) ice sheets to present-day sea-level rise of ~1.8 mm/year (*5*). Rapid increases in near-coastal Greenland ice-sheet thinning (*2*) and West Antarctic glacial discharge (*4*) strengthen concern about accelerated sea-level rise caused by ice-sheet change. In contrast, the latest Intergovernmental Panel on Climate Change (IPCC) assessment predicts that overall, the Antarctic ice sheet will absorb mass during the 21st century due to increased precipitation in a warming global climate (*6*). Thus, increased precipitation over Antarctica could mitigate some of the mass loss from other terrestrial ice sources and their contributions to global sea-level rise. Here, we analyze elevation change of the Antarctic ice-sheet interior from 1992 to 2003 using nearly continuous satellite radar altimeter measurements. Because temporal variations in snowfall have been linked previously to decadal elevation change in Greenland's interior (*7*), we compare the observed elevation change to newly released meteorological model estimates of contemporaneous snowfall.

After correction for isostatic uplift, ice-sheet elevation-change measurements from continuous and/or repeat altimeter surveys are a direct measure of net mass change. We measured elevation change (*dH*) over 8.5 million km^2 of the grounded Antarctic ice-sheet interior (~70% of total ice-sheet area) using ~347 million *dH* measurements derived from European Remote-Sensing Satellite–1 (ERS-1) and ERS-2 ice-mode satellite radar altimeter data (coverage extends to 81.6°S). These data were processed and analyzed in a manner consistent with the procedures and methods described in (*8*–*10*). We generated time series (Fig. 1) of monthly *dH* averages from 1992 to 2003 for ~1500 1° × 2° (latitude × longitude) regions, 22 major drainage basins, Berkner Island, West and East Antarctica, and the entire region of coverage (ROC) (*11*).

The *dH* time series were fit with an autoregressive (AR) model superimposed upon a longer-term trend (Fig. 1). We used the AR model to characterize seasonal and interannual variations in the elevation-change time series (*8*). The long-term trend was modeled as a polynomial that was estimated from a smoothed version of the time series generated by an iterative local average filter (*10*). We estimated the average rate of elevation change (*dH/dt*) during the 11-year period by a least-squares fit to the long-term polynomial trend and then corrected for isostatic uplift (*12*). The 11-year elevation-change results (Fig. 2) show that the vast majority of regions in East Antarctica are thickening, especially in the interior, whereas regions in West Antarctica exhibit both strong thickening and thinning trends. At the basin scale, *dH/dt* values range from 0 to +6 cm/year for East Antarctica, whereas there is substantial spatial variability in West Antarctica, with *dH/dt* values ranging from –10 to +19 cm/year (table S1). The coarse spatial coverage of satellite radar altimetry compromises its utility as a tool to map elevation changes in steeply sloped coastal regions, so these results only address the average elevation change of the Antarctic ice-sheet interior within the ROC.

The dominant characteristic in East Antarctica is the large and spatially coherent area of slight thickening throughout the interior. Also noteworthy is the area with moderate thickening south and east of the Amery ice shelf in basin B-C, which changes to strong thickening in the near-coastal area of basin C-C′ east of the Amery ice shelf. Overall, the East Antarctic ice-sheet interior within the ROC is thickening at a rate of 1.8 ± 0.3 cm/year. In contrast, the West Antarctic ice sheet exhibits bimodal behavior. There is modest to strong thinning in the basins of Marie Byrd Land (E″-H). Strong thinning in basin G-H is associated with even more rapid thinning in the coastal outlets of the Pine Island and Thwaites glaciers (*4*, *9*, *13*), possibly caused by increased basal melting due to ocean thermal forcing (*14*). Conversely, basins adjacent to the Antarctic Peninsula and Ronne ice

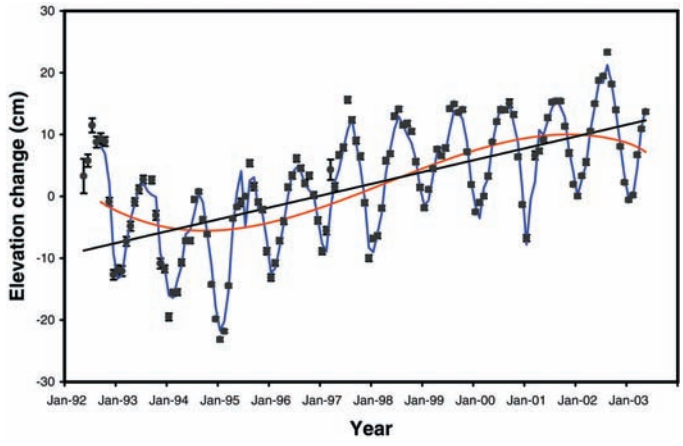

Fig. 1. Elevation-change (black circles) time series from 1992 to 2003 for ~7.1 × 10^6 km^2 of the East Antarctic ice-sheet interior. The seasonal and interannual cycle (blue line) and long-term trend (red line) are modeled as described in the text. The average rate of change (black line) for the entire time period is 1.8 cm/year after adjustment for isostatic uplift. A steady increase in elevation since about 1995 is apparent. The average rate of change from 1995 to 2003 is 2.2 cm/year after adjustment for isostatic uplift.

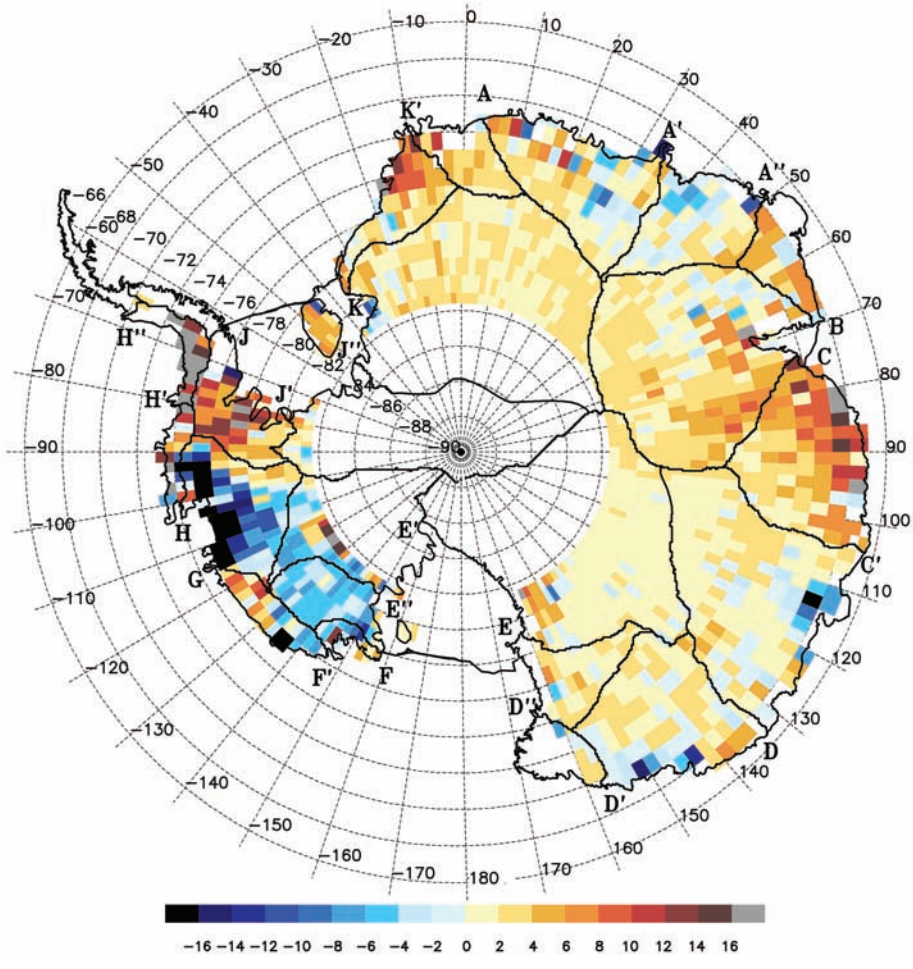

Fig. 2. Elevation-change rate (cm/year) from 1992 to 2003 for 8.5 × 10^6 km^2 of the grounded Antarctic ice-sheet interior. Results are shown in 1° × 2° (latitude × longitude) regions, and boundaries of major drainage basins discussed in the text are superimposed.

[1]Department of Electrical and Computer Engineering, University of Missouri–Columbia, Columbia, MO 65211, USA. [2]Desert Research Institute, University and Community College System of Nevada, Reno, NV 89512, USA. [3]Department of Hydrology and Water Resources, University of Arizona, Tucson, AZ 85721, USA. [4]Department of Geography, University of Sheffield, Sheffield S10 2TN, UK.

*To whom correspondence should be addressed. E-mail: davisch@missouri.edu

shelf (basins H-H′, H′-H″, J-J′) show strong thickening of between 8 and 19 cm/year. However, these regions represent only ~30% of the area of the West Antarctic ice sheet within the ROC, so the overall trend is slight thinning in the interior of 0.9 ± 0.3 cm/year.

Elevation-change results for West Antarctica, East Antarctica, and the ROC are significantly more positive than previously reported for the time period from 1992 to 1996 (*15*). In East Antarctica, this is due primarily to a steady increase in elevation that began in 1995 (Fig. 1). In West Antarctica, this is due to both an increase in spatial coverage for these results (basins H-H′, H′-H″, and J-J′) and a near-zero rate of overall elevation change since 1997, as compared to a more negative overall trend in the preceding years. For the ROC, the 5:1 ratio in East versus West Antarctic area coverage causes slight thickening overall at the rate of 1.4 ± 0.3 cm/year.

Interpretation of elevation-change measurements requires precise knowledge of contemporaneous changes in snowfall because temporal snowfall variations can cause interannual-to-decadal or longer fluctuations in ice-sheet elevation (*7*). Because we have no direct precipitation measurements exactly spanning the time period of the altimetry measurements, we used newly released 1980 to 2001 ERA-40 reanalysis from the European Centre for Medium-Range Weather Forecasts (ECMWF) together with 2002 to 2003 ECMWF operational analyses to evaluate overall temporal trends in snowfall (Fig. 3) during the altimetry measurement period (*11*).

In East Antarctica, the modeled spatial patterns of average snowfall change broadly match the *dH/dt* results derived from radar altimetry, suggesting that much of the 1992 to 2003 elevation change may be linked to changes in snow accumulation. These include many of the dominant elevation-change features observed during the 1992 to 2003 period (Fig. 2). Specifically, the modeled snowfall trend matches the large and coherent area of slight thickening throughout the interior, slight to moderate thinning in the coastal areas of southeastern Queen Maud Land (basin A′-A″) and King George V Land (basin D-D′), moderate thickening for northern Coats Land (basin K-K′), and strong thickening for King Wilhelm II Land (basin C-C′). For East Antarctica, the linear correlation between observed 1992 to 2003 elevation-change trends and modeled snowfall trends is 0.41 ($P \leq 0.01$) at the 1° × 2° region scale and 0.85 ($P \leq 0.01$) at the basin scale (*11*).

Agreement between the spatial patterns is much lower for West Antarctica where changes due to ice dynamics can be substantial (*3*). Comparisons suggest, however, that some of the observed bimodal *dH/dt* behavior may be due to recent snowfall changes. Specifically, the strong thickening observed in basins H′-H″ and J-J′ corresponds to regions with positive snowfall trends. In addition, modest thickening is observed in both trends over Berkner Island. Although there is some general thinning apparent in both maps for the interior areas of E′-E″, E″-F, and G-H, there are strong differences in the coastal areas of F-G, G-H, and H-H′. Consequently, the linear correlation between observed *dH/dt* and modeled snow-precipitation trends is 0.11 for individual 1° × 2° regions and 0.25 for basin trends. Neither is significant at the 90% confidence interval.

Elevation-change rates estimated from model-derived snowfall trends are much smaller than the observed *dH/dt* values, even though the spatial patterns are similar in East Antarctica. To investigate this difference, we compared spatial and temporal variability in snowfall from the ERA-40 and ECMWF models to point observations from ice-core measurements and regional estimates of snow accumulation from remote sensing. Similar prior comparisons in Greenland show that ERA-40 reanalysis closely simulates the relative temporal variability in snow accumulation observed in ice cores (*16*). As with other meteorological models of Greenland precipitation, however, ERA-40 reanalysis predicts too little snowfall in the interior of the ice sheet (*17*, *18*).

Although snowfall rates for much of the Antarctic interior are too low to allow annual-layer preservation in glaciochemical signals, annual snow accumulation can be measured in ice cores from much of West Antarctica. We used 20 ice-core records to evaluate meteorological model estimates of snow accumulation (*11*) in West Antarctica located within or very near basins G-H and E′-E″ (Fig. 3). Linear correlations between the standardized ensembles of model-simulated and observed annual snowfall at the core sites are 0.55 ($P \leq 0.01$) and 0.68 ($P \leq 0.01$) during the period 1980 to 2001 and 0.62 ($P \leq 0.10$) and 0.91 ($P \leq 0.01$) during the period 1992 to 2001 for basins G-H and E-E″, respectively.

Mean annual snowfall rates estimated from the model, however, were only 83% of observed rates for the core sites in basin G-H and 66% for the more interior sites in basin E′-E″. At the South Pole and very arid sites on the polar plateau where annual glaciochemical layers are not preserved, mean snow accumulation from the reanalysis is only 20 to 60% of

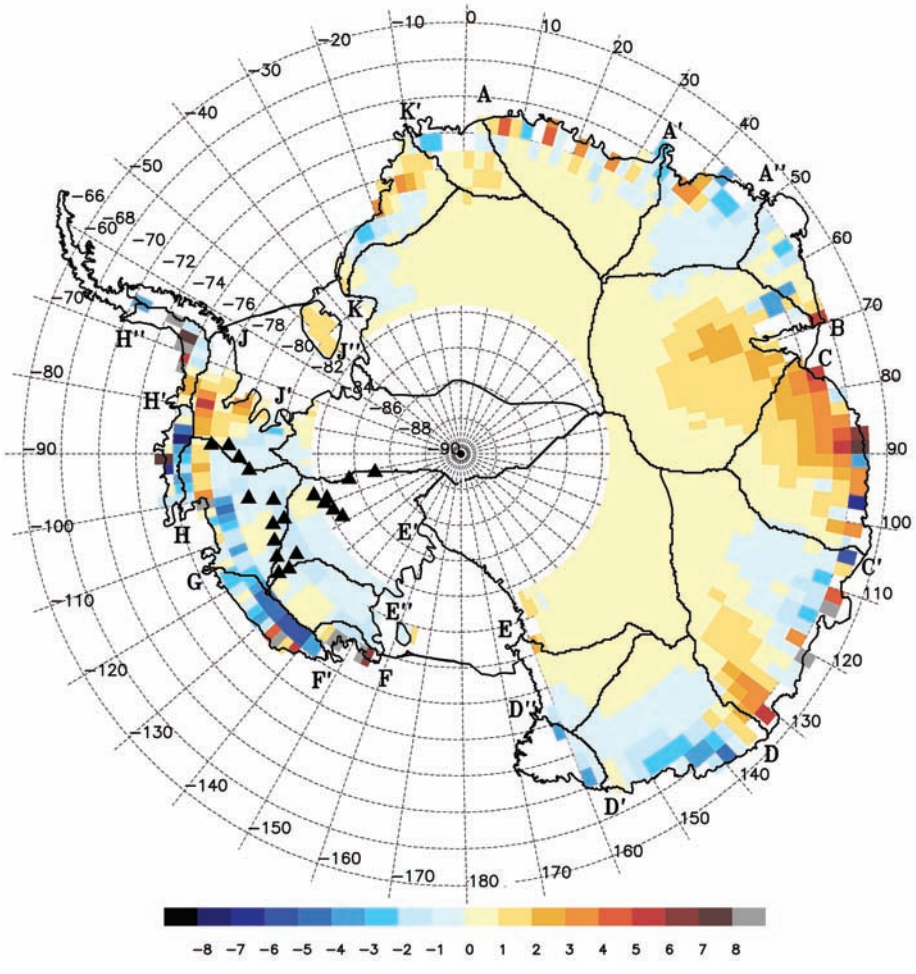

Fig. 3. Precipitation change (cm of snow per year) from 1992 to 2003 corresponding to elevation-change area coverage in Fig. 2. Ice-core locations (black triangles) discussed in the text are also shown.

observed rates. Comparisons at regional to continental scales also show that mean snow accumulation from meteorological models is very low over most of the interior of the Antarctic continent. For example, basin-averaged, model-simulated, mean-annual snow accumulation compared with regional accumulation estimates compiled from in situ and passive microwave measurements (*19*) ranged from 25 to 50% for primarily interior basins (e.g., J″-K and B-C).

It is clear, therefore, that the ERA-40 reanalysis and ECMWF operational analyses used here capture much of the relative temporal variability in accumulation while underestimating the total amount, resulting in underestimation of the magnitude of modeled temporal trends in snowfall rate. Although some of the difference between observed elevation change and modeled snowfall-rate trends likely results from changes in snow densification in response to changing snow accumulation rate and temperature (*20*), most of the difference probably results from underestimation of the magnitude of annual-to-decadal changes in snowfall by the meteorological models.

Placing these results in perspective, a sea-level change of 1 mm/year corresponds to 360 billion metric tons of water per year (*21*). Using a near-surface snow density of 350 kg/m^3, an average elevation change of 1.8 ± 0.3 cm/year over an area of 7.1 million km^2 for the East Antarctic interior (table S1) corresponds to a mass gain of 45 ± 7 billion metric tons of water per year and a corresponding sea-level drop of 0.12 ± 0.02 mm/year. We believe that this is a conservative estimate. The spatially uniform and positive *dH/dt* values for the East Antarctic interior (Fig. 2) suggest that much of the area south of the East Antarctic ROC may also be thickening. These results are consistent with ice-core evidence, though sparse, for increasing accumulation in East Antarctica during the decades preceding our observational time period (*22*–*26*). Thus, we cannot rule out a longer-term mass imbalance due to increased precipitation, as predicted by earlier studies [e.g., (*27*, *28*)] and the most recent IPCC assessment (*6*).

The vast size of the East Antarctic ice sheet means that even a small imbalance has a large effect on sea-level change. For example, a 1.8 cm/year average *dH/dt* over the entire East Antarctic ice sheet (~10 million km^2) would correspond to a sea-level drop of 0.18 mm/year (assuming a recent change and snow density of 350 kg/m^3), nearly as large as the most recent estimate of 0.20 mm/year (*2*) for the Greenland ice sheet's contribution to sea-level rise, and larger than the most recent estimate for the West Antarctic ice sheet's contribution of 0.16 mm/year (*3*).

Our results show that the East Antarctic ice-sheet interior increased in overall thickness within the ROC from 1992 to 2003 and that this increase is probably the result of increased snowfall. Both of these observations are consistent with the latest IPCC prediction for Antarctica's likely response to a warming global climate (*6*). However, the IPCC prediction does not consider possible dynamic changes in coastal areas of the ice sheet. Moreover, these results have only sparse coverage of the coastal areas where recent dynamic changes may be occurring (*4*). Thus, the overall contribution of the Antarctic ice sheet to global sea-level change will depend on the balance between mass changes on the interior and those in coastal areas.

References and Notes

1. W. Krabill *et al.*, *Science* **289**, 428 (2000).
2. W. Krabill *et al.*, *Geophys. Res. Lett.* **31**, L24402 (2004).
3. E. Rignot, R. Thomas, *Science* **297**, 1502 (2002).
4. R. Thomas *et al.*, *Science* **306**, 255 (2004).
5. Intergovernmental Panel on Climate Change, *IPCC Third Assessment Report, Climate Change 2001: The Scientific Basis* (Cambridge Univ. Press, Cambridge, 2001).
6. J. A. Church *et al.*, in *Climate Change 2001: The Scientific Basis* (Cambridge Univ. Press, Cambridge, 2001), pp. 639–694.
7. J. R. McConnell *et al.*, *Nature* **406**, 877 (2000).
8. A. C. Ferguson, C. H. Davis, J. E. Cavanaugh, *IEEE Trans. Geosci. Remote Sens.* **42**, 2426 (2004).
9. C. H. Davis, A. C. Ferguson, *IEEE Trans. Geosci. Remote Sens.* **42**, 2437 (2004).
10. Y. Li, C. H. Davis, Proceedings of the 2005 International Geoscience and Remote Sensing Symposium, Seoul, South Korea (Institute of Electrical and Electronics Engineers, Piscataway, NJ), in press.
11. Materials and methods are available as supporting material on *Science* Online.
12. E. R. Ivins, X. Wu, C. A. Raymond, C. F. Yoder, T. S. James, *Int. Assoc. Geodesy Symp.* **123**, 361 (2001).
13. A. Shepherd, D. J. Wingham, J. A. D. Mansley, H. F. J. Corr, *Science* **291**, 862 (2001).
14. E. Rignot, S. Jacobs, *Science* **296**, 2020 (2002).
15. D. J. Wingham, A. J. Ridout, R. Scharroo, R. J. Arthern, C. K. Shum, *Science* **282**, 456 (1998).
16. E. Hanna, J. R. McConnell, S. Das, J. Cappelen, A. Stephens, *J. Clim.*, in press.
17. J. R. McConnell *et al.*, *J. Geophys. Res.* **40**, 605 (1998).
18. Q. S. Chen *et al.*, *J. Clim.* **10**, 839 (1997).
19. D. G. Vaughan, J. L. Bamber, M. Giovinetto, J. Russell, A. P. R. Cooper, *J. Clim.* **12**, 933 (1999).
20. R. J. Arthern, D. J. Wingham, *Clim. Change* **40**, 605 (1998).
21. S. S. Jacobs, *Nature* **360**, 29 (1992).
22. V. I. Morgan, I. D. Goodwin, D. M. Etheridge, C. W. Wookey, *Nature* **354**, 58 (1991).
23. E. Mosley-Thompson *et al.*, *Ann. Glaciol.* **21**, 131 (1995).
24. E. Mosley-Thompson, J. F. Paskievitch, A. J. Gow, L. G. Thompson, *J. Geophys. Res.* **104**, 3877 (1999).
25. J. Wen *et al.*, *Polar Meteorol. Glaciol.* **15**, 43 (2001).
26. I. Goodwin, M. de Angelis, M. Pook, N. W. Young, *J. Geophys. Res.* **108**, 4673 (2003).
27. J. Oerlemans, *J. Clim.* **2**, 1 (1982).
28. P. Huybrechts, J. Oerlemans, *Clim. Dyn.* **5**, 93 (1990).

29. ERA-40 and ECMWF operational analysis data were provided by A. Stephens (British Atmospheric Data Centre). This work was supported by NASA's Cryospheric Processes Program (C.H.D., Y.L., and J.R.M.) and the NSF Antarctic Glaciology Program (J.R.M. and M.M.F.). We thank the U.S. ITASE field team, R. Kreidberg for help with the manuscript, and two anonymous reviewers for comments that improved this manuscript.

Supporting Online Material

www.sciencemag.org/cgi/content/full/1110662/DC1
Materials and Methods
Figs. S1 to S4
Table S1
References and Notes

3 February 2005; accepted 5 May 2005
Published online 19 May 2005;
10.1126/science.1110662
Include this information when citing this paper.

Cleaning the Air and Improving Health with Hydrogen Fuel-Cell Vehicles

M. Z. Jacobson,[1]* W. G. Colella,[1] D. M. Golden[2]

Converting all U.S. onroad vehicles to hydrogen fuel-cell vehicles (HFCVs) may improve air quality, health, and climate significantly, whether the hydrogen is produced by steam reforming of natural gas, wind electrolysis, or coal gasification. Most benefits would result from eliminating current vehicle exhaust. Wind and natural gas HFCVs offer the greatest potential health benefits and could save 3700 to 6400 U.S. lives annually. Wind HFCVs should benefit climate most. An all-HFCV fleet would hardly affect tropospheric water vapor concentrations. Conversion to coal HFCVs may improve health but would damage climate more than fossil/electric hybrids. The real cost of hydrogen from wind electrolysis may be below that of U.S. gasoline.

Switching from a fossil-fuel economy to a hydrogen economy would be subject to technological hurdles, the difficulty of creating a new energy infrastructure, and considerable conversion costs (*1*) but could provide health, environmental, climate, and economic benefits and reduce reliance on diminishing oil supplies. Although studies have modeled the effects of hydrogen leakage or reduced emission on global tropospheric and stratospheric chemistry (*2*–*4*), no study has examined the effect on urban pollution or health of establishing a hydrogen economy. Furthermore, no study has examined the likely effects of this switch on aerosol particles (which have a large impact on climate and are the deadliest components